Effect of Glass Bead Content and Diameter on Shrinkage and Warpage of Injection-Molded PA6

J.G. Kovács, B. Solymossy

Department of Polymer Engineering, Budapest University of Technology and Economics,
H-1111 Budapest, Műegyetem rkp. 3., Hungary

A simple technique has been introduced to evaluate the shrinkage and warpage behavior of injection molded products. Using the shrinkage values measured on specific locations of the specimen, three deformation factors have been defined to characterize the warpage behavior of the materials examined. Experiments were carried out to determine these properties of injection molded polyamide 6 (PA6) composites with solid glass bead (GB) contents of 10, 20, 30, 40 wt% and diameters of 11, 85, 156, 203 μm. It was concluded that the flow directional shrinkages can principally be described by the change in the bead content and diameter; it was proven that the increase in bead content and in bead diameter induces a reduction in flow directional shrinkage. The rising bead content and diameter increased the deformation factor, defined by the shrinkage differences caused by the pressure drop. It was pointed out that the ideal bead content can be determined in the function of bead diameter. POLYM. ENG. SCI., 49:2218–2224, 2009. © 2009 Society of Plastics Engineers

INTRODUCTION

One of the most important properties of parts produced with injection molding—being the most widespread technique for processing polymers—is their dimensional accuracy. It can be easily seen that a deviation from the accepted tolerance range of the part can lead to the dismissal of the complete series produced. This attribute of polymeric materials to change their volume during—and after—processing is called shrinkage. According to Jansen et al. [1], there are three types of shrinkages: in-mold shrinkage, which happens during processing, as-molded shrinkage (or mold shrinkage taking place after the mold is opened), and postmold shrinkage (long time shrinkage caused by physical aging and recrystallization of the part) [2, 3]. In most studies, according to the relevant standards (DIN 16901, ISO 294-4), shrinkage was measured at 24 or 48 h after production [1, 4–6]. Some researchers adopted measurement points at 168 h [7, 8] or later to examine the post shrinkage of their products.

The uneven shrinkage and warpage can be attributed to numerous parameters from among which the most significant are the followings: differential cross-flow and parallel to flow shrinkages, shrinkages caused by uneven cooling, anisotropic material properties, and shrinkages caused by thermal stresses [9, 10]. Numerous investigations have been carried out to examine the effecting factors of shrinkage in unfilled thermoplastics [1, 3, 5]. Depending on the material used—amorphous or semi-crystalline—the values of flow directional and cross-flow shrinkages differ. In most cases, the studies pointed out that cross-flow shrinkage is larger than the flow directional shrinkage, an exception was Thomas' and Caffery's work [11] where this proportion turned over near the gate using polypropylene (PP). Shelesh-Nezad and Taghizadeh [6] learned that the shrinkage difference in flow and cross-flow directions of pure PP was 14% (1.64% shrinkage in the flow direction when compared with 1.41% in the cross-flow direction) and the addition of talc mineral filler (30 wt%) induced an isotropic shrinkage in the molded part. According to Shay et al. [12], significant difference concerning the two shrinkages was not found using amorphous materials. With semi-crystalline materials, Postawa and Koszkul [3] had observed an 8–10% difference between shrinkages of the two mentioned directions. Almost all research groups agreed—examining a given geometry—on that the holding pressure had the most significant effect on the shrinkage of the part [1, 5, 7]. By increasing the holding pressure, the decrease of the shrinkage was observed. According to Postawa and Koszkul, the second most important processing parameter was injection temperature the change of which modified the melt viscosity [3]. By increasing the temperature, a better pressure distribution along the flow path was noticed, causing a reduction in shrinkage. With longer holding times, shrinkage values were reduced until the gate freeze-off was reached.

In the case of reinforced or filled injection moldings, several studies dealt with different fiber reinforcements. These studies concluded that the reinforcement decreased the shrinkage in the flow direction in a higher degree than in the cross-flow direction causing the so-called warpage of the part. According to Jansen et al., a typical value for fiber reinforced shrinkage in the flow direction was 0.2%, whereas the reduction of cross-flow shrinkage was reduced negligible [1]. DePolo and Baird [13] found that 6 mm long pregenerated thermotropic liquid crystalline polymer (TLCP) microfibrils (from 0 to 40 wt%) significantly increased (from 3% to 18%) the warpage of their PP parts while reducing the value of the flow directional shrinkage by 1% and the cross-flow shrinkage by 0.3%. With the application of fillers instead of fibers, a smaller degree of shrinkage reduction in the flow direction was experienced, but the difference between the flow directional and cross-flow shrinkages was significantly reduced. Mamat et al. [5]—using unfilled and 40 wt% calcium carbonate ($CaCO_3$)-filled PP—experienced a reduction (from 1.8% to 1.6%) in the cross-flow shrinkage and in the difference between the two shrinkages of the part.

Several studies dealt with glass beads, however, the majority of them examined the effect on the rheological [14–16] and mechanical properties [17–19] and some on the morphology developed [20–22]. Both studies agreed on that the glass bead content raises the viscosity of the melt; moreover, the viscosity is in direct proportion with the glass bead content. This effect is increased by decreasing the shear rate. In most cases with increasing the bead content, a rise in the modulus of elasticity, the decrease of the elongation at break, and the fall of tensile stress is experienced. The bead diameter does not have a significant effect on the mentioned mechanical properties of the material. Some investigations were carried out to examine the effect of solid glass beads on the shrinkage of injection molded thermoplastics [18]. But these studies were dealing mostly with bead content, leaving the effect of bead size out from the examination range. Huang et al. [18] for example examined the effect of different bead content (0, 5, 20, and 25 wt%) on the shrinkage of micro-injection-molded products and seen that it was inverse proportional to the shrinkage of their parts; the application of 25 wt% glass bead reduced the shrinkage of the part from an initial value of 2.8% to 1.3%.

In spite of the numerous studies dealing with glass beads, relatively few examined the effect of fillers on the shrinkage properties of the materials and none of them examined the effect of bead size. According to the previous studies in the field of segregation [23–25], an effect of the bead size and content on the shrinkage of the part was expected. In this way, the objective of this article is to present a simple technique to evaluate the shrinkage and warpage of injection-molded products. For this purpose, solid glass bead-filled PA6 with varying bead diameters and contents were used.
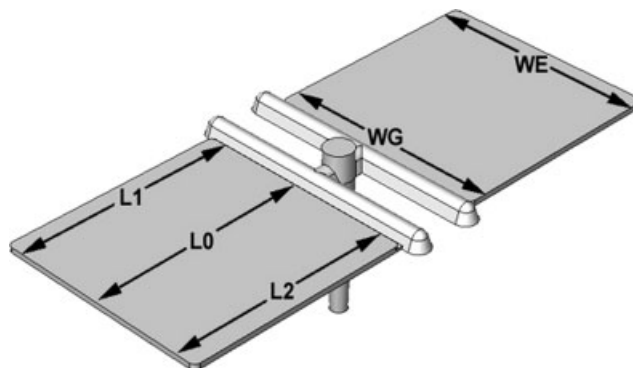

FIG. 1. The injection molded specimens with the shrinkage measuring points (L_0 – the length of the specimen in the middle, L_1 and L_2 – the length of the specimen at the edge, W_G – the width of the specimen next to the gate, W_E – the width of the specimen far from the gate).

EXPERIMENTAL

PA6 matrix filled with solid glass beads of different diameter (11, 85, 156, 203 μm) and content (10, 20, 30, 40 wt%) were examined in this study. The matrix (Lanxess, Durethan B30S) and the beads (Potters Industries Inc., Spheriglass® with coupling agent) were mixed on a Brabender Plasticorder 814402 type twin-screw extruder with constant screw revolutions per minute. A Brabender pelletizer was used to produce pellets from the extrudate. The glass bead contents of each material was verified by determining the ash content where the maximum deviation was 3.7 wt% from the nominal values. From these materials, 80 $\times$ 80 $\times$ 2 mm specimens (Fig. 1) were injection molded on an Arburg 320C 600–250 injection molding machine with the following injection molding parameters (Table 1).

During the injection molding, a uniform filling pattern was adopted. Five measurement locations were marked on each specimen where the appropriate dimensions (Fig. 1) were measured with a Mitutoyo digital caliper—with two decimal digit precision—at 1 min, 1 h, 4 h, 24 h, and 168 h after demolding. To prevent moisture absorption, the specimens were stored under room temperature and were subjected to predried silica gel between the measurements. From the measured dimensions of the specimens and the nominal dimensions of the cavity—measured at room temperature—the linear shrinkages were determined according to (1):

$$S_i = \frac{L_M \cdot L_i}{L_M} \cdot 100 [\%], \qquad (1)$$

where S_i [%] is the shrinkage in percentage, L_M [mm] is the dimension of the cavity, and L_i [mm] is the relating measured dimension of the specimen.

TABLE 1. The injection molding parameters.

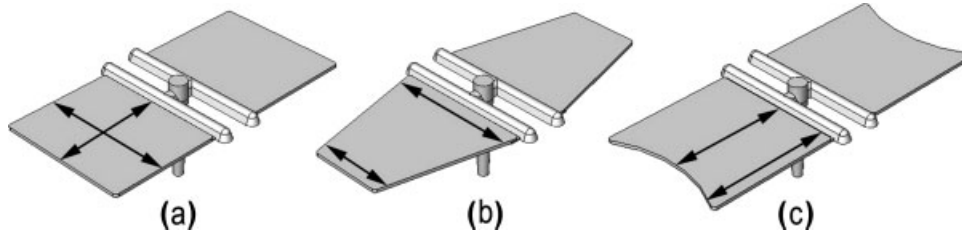| Melt temperature	Mold temperature	Volumetric flow rate
280°C	80°C	50 cm³/s

FIG. 2. Deformations defined by the three deformation factors (a) deformation factor defined by the cross-flow direction and the flow directional shrinkages (DFWL), (b) deformation factor defined by the pressure drop caused shrinkage differences (DFP), (c) deformation factor defined by the flow directional shrinkage differences (DFL).

The average flow directional shrinkage at the edge of the specimen is as follows:

$$S_{LE} = \frac{S_{L1} + S_{L2}}{2} [\%], \qquad (2)$$

where S_{LE} [%] is the average flow directional shrinkage at the edge of the specimen, S_{L1} [%] and S_{L2} [%] are the flow directional shrinkages at the two sides in flow direction of the specimen.

The mean cross-flow direction and flow directional shrinkages are as follows:

$$S_W = \frac{S_{WG} + S_{WE}}{2} [\%], \qquad (3)$$

$$S_L = \frac{S_{L0} + S_{LE}}{2} [\%], \qquad (4)$$

where S_W [%] is the average cross-flow direction shrinkage, S_L [%] is the average flow directional shrinkage, S_{WG} [%] is the cross-flow direction shrinkage near the gate, S_{WE} [%] is the cross-flow direction shrinkage at the end of the flow, S_{L0} [%] is the flow directional shrinkage in the center in flow direction of the specimen, and S_{LE} [%] is the mean flow directional shrinkage at the edge of the specimen.

According to Kovács and Tábi, three deformation factors were used to describe the warpage caused by inho-

mogeneous shrinkage [26]. These deformation factors were defined using the measured shrinkages of the specimens shown on Fig. 1:

Deformation factor defined by the cross-flow direction and the flow directional shrinkages (Figs. 1 and 2a):

$$DFWL = \frac{S_W}{S_L} [-], \qquad (5)$$

Deformation factor defined by the pressure drop caused shrinkage differences (Figs. 1 and 2b):

$$DFP = \frac{S_{WG}}{S_{WE}} [-], \qquad (6)$$

Deformation factor defined by the flow directional shrinkage differences (Figs. 1 and 2c):

$$DFL = \frac{S_{L0}}{S_{LE}} [-]. \qquad (7)$$

The ideal value of these factors is 1, when the shrinkages in the numerator and in the denominator are equal.

RESULTS AND DISCUSSION

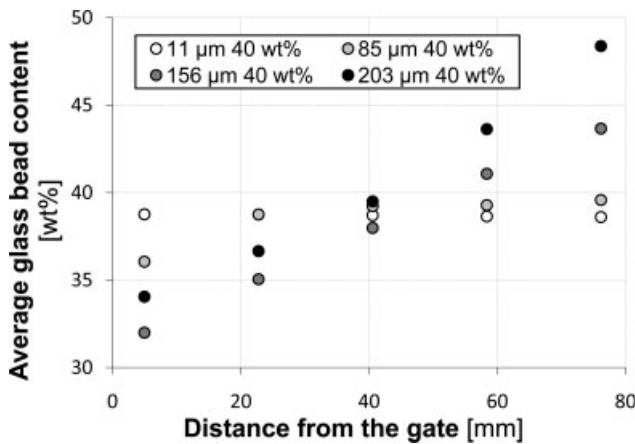As a result of the measurements, it can be seen that regardless of bead size and content the curves for different

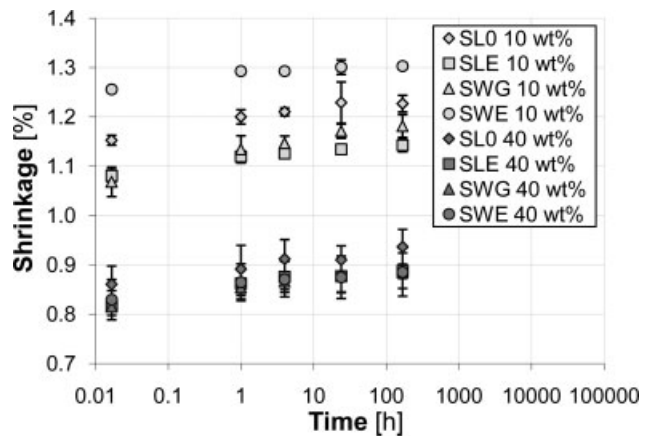FIG. 3. Inhomogeneous filler distribution along the flow path.

FIG. 4. Shrinkage in function of time (bead diameter 11 μm and content of 10 and 40 wt%).
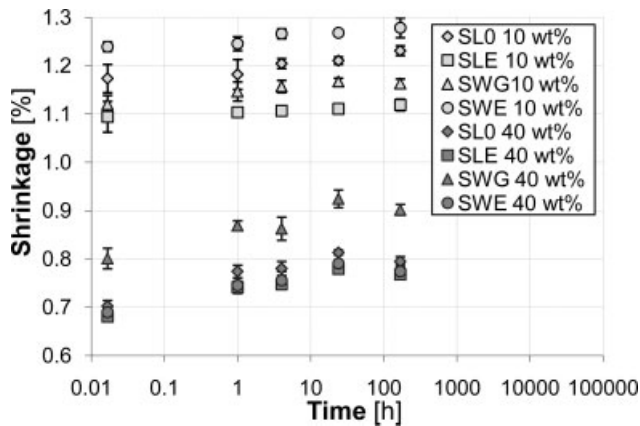
FIG. 5. Shrinkage in the function of time (bead diameter 203 μm and content 10 and 40 wt%).

FIG. 7. Cross-flow direction shrinkage at the end of the flow, 24 h after injection molding in the function of glass bead content and size.

shrinkages preserved their characteristics. The raising bead content decreased the shrinkages. Furthermore, the differences between the shrinkages measured in different directions became smaller, moving the corresponding deformation factor values closer to 1. At low bead content levels, the cross-flow direction shrinkage at the end of the flow (S_{WE}) had the highest values, probably because of the pressure drop along the melt flow. At high bead content levels and large bead sizes, the two cross-flow direction shrinkages change places and the cross-flow direction shrinkage near the gate becomes higher. This phenomenon can be explained by segregation [25, 27, 28]. With higher filler content and larger filler size, the local filler content rises at the end of the flow path and decreases near the gates, thereby changing the viscosity of the melt too (Fig. 3).

By creating an inhomogeneous viscosity along the flow path, the pressure distribution was also changed. The bead content acts in the opposite direction as the pressure drop and decrease the shrinkage at the end of the flow path but decrease it with a smaller degree near the gates. It can be seen that at larger bead sizes and higher bead contents the
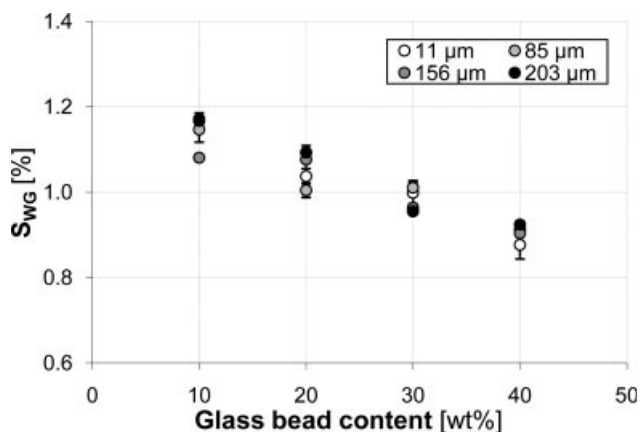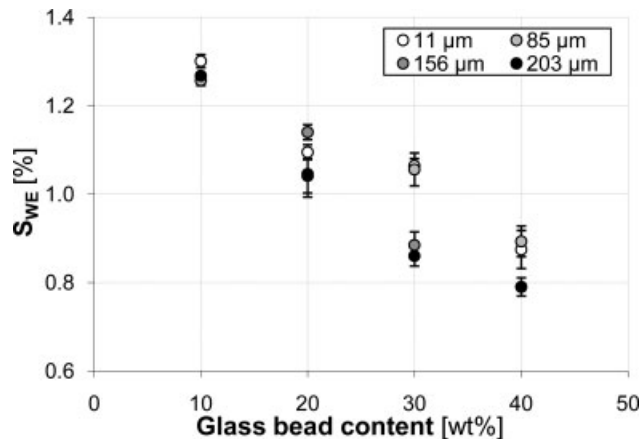
values for the different kinds of shrinkages were lower than at smaller sizes and contents (Figs. 4 and 5).

It can be seen that the bead size had no effect on the shrinkage near the gate but affected the shrinkage at the end of the flow. It can be explained by the change in the flow ability that affects the pressure distribution of the material (Figs. 6 and 7).

Time Dependent Shrinkage

Flow directional shrinkages have shown a large deviation in time, as a function of glass bead content (Fig. 8).

Based on these measurements, a simple formula has been proposed to describe the relation between the changes of flow directional shrinkage in time, glass bead size, and content:

$$S_L(t) = A_{SL} \cdot \ln(t) + \left(S_{Lt0} - \frac{x}{C_{SL} \cdot db - C_{SL0}} \right) [\%] \quad (8)$$

where $S_L(t)$ [%] is the flow directional shrinkage in the function of time, A_{SL} [−] and C_{SL} [−] are material depend-

FIG. 6. Cross-flow direction shrinkage near the gate, 24 h after injection molding in the function of glass bead content and size.
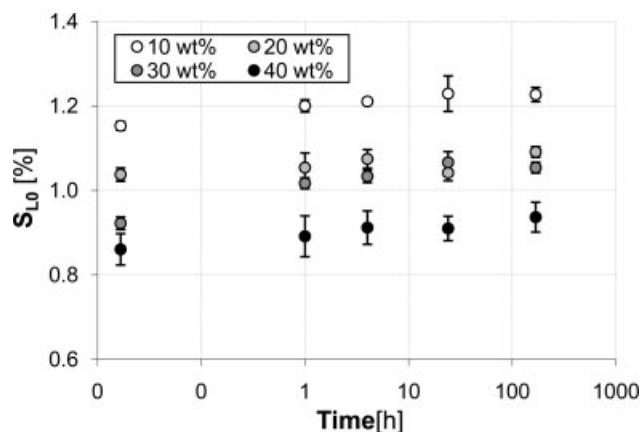

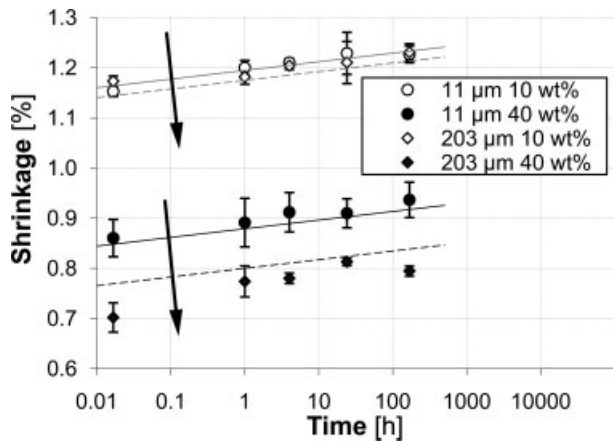FIG. 8. Flow directional shrinkages in the function of time (bead diameter 11 μm).

FIG. 9. Flow directional shrinkage in the function of time and bead size (11 and 203 μm), based on measured (points) and calculated data (trends).

FIG. 10. Deformation factor defined by the flow directional shrinkage differences in function of glass bead content and size.

ent parameters, C_{SL0} [–] is a constant for the unfilled material, x [wt%] is the glass bead content, d_b [μm] is the glass bead diameter, and S_{Lt0} [%] is the flow directional shrinkage of the unfilled material measured 1 h after the injection molding.

The trends show a good relation with the measurements. It can be seen on the figure that the application of larger beads decreased the shrinkage values consequently further increasing the distance between the curves with higher glass bead content (Fig. 9).

The relation's (8) validity was proven only in the range of investigation, meaning a glass bead content range of 10–40 wt%, a duration of 0.016–168 h and a glass bead size range of 11–203 μm. Table 2 contains the assessed values of the parameters featured in *Eq. 8*. By statistically evaluating the suitability of the data, the value of the correlation coefficient was (R^2) 0.97.

Deformation Attributes

Regarding to injection molded products, it is more important that uniform shrinkage is achieved, namely the deformation of the product is reduced. The previously introduced deformation factors are appropriate to characterize these warpage properties. The deformation factor defined by the flow directional shrinkage differences indicates the changes of the shrinkages along the flow path. It was concluded that neither the glass bead content nor the size has any effect on the value of this factor, so the shrinkages (L_0, L_1, and L_2) reacted to a similar degree to the changes of the main parameters (Fig. 10).

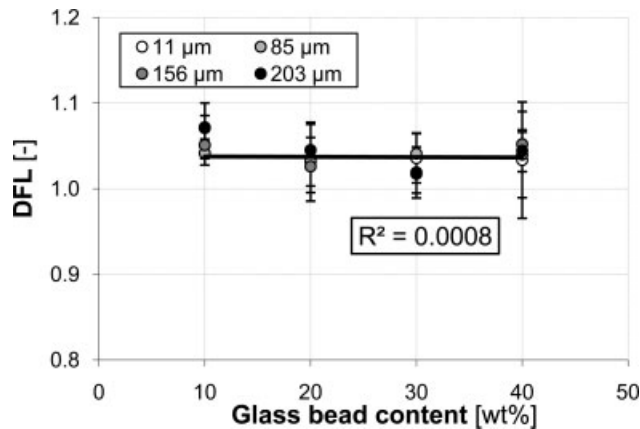The deformation factor, defined by the cross-flow direction and the flow directional shrinkages (DFWL, *Eq.*

5) characterizes the deformations derived from the melt flow. The value of this factor, which can easily be raised by the application of glass fibers, can be considerably lowered by the use of glass beads. It can be seen on the following figure that with raising glass bead content and decreasing bead size the factor's value can be moved to the direction of its ideal value (Fig. 11).

The pressure dependence of shrinkage is a minor research area, although it has an important role in the deformation of injection molded products. The previously introduced deformation factor defined by the pressure drop caused shrinkage differences is the index-number for characterizing this attribute. The increase of DFP was experienced with the raising of bead content and diameter (Fig. 12). This relation was described with the following equation:

$$\text{DFP} = (m_b \cdot d_b + m_0) \cdot x + \text{DFP}_0 \; [-] \tag{9}$$

where DFP [–] is the deformation factor defined by the pressure drop caused shrinkage differences, m_b [–] and m_0
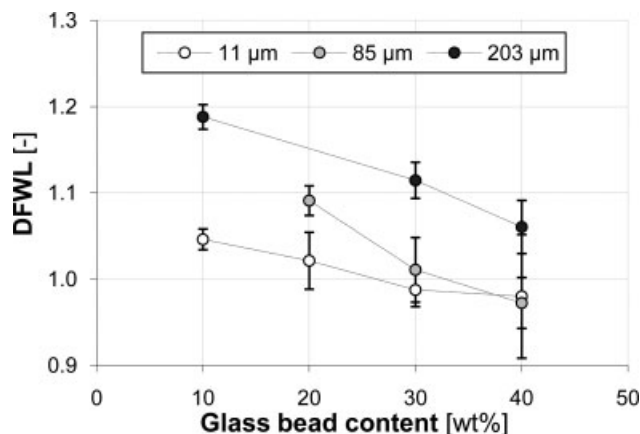

FIG. 11. Deformation factor defined by the cross-flow direction and the flow directional shrinkages in function of glass bead content and size.

TABLE 2. Parameters of glass bead filled PA6 (Durethan B30S).

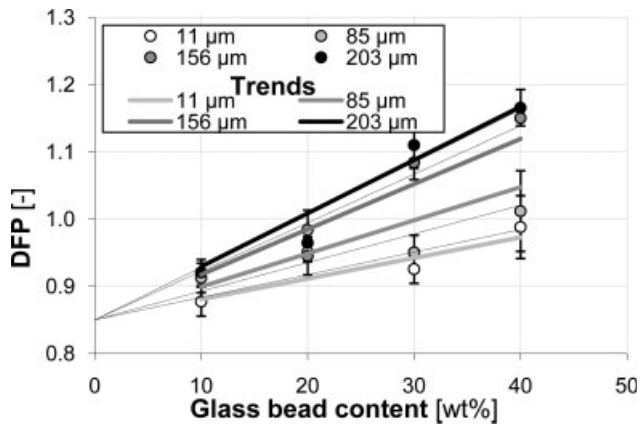| SL_{t0}	A_{SL}	C_{SL}	C_{SL0}
1.3	0.0075	−0.0765	96.2

FIG. 12. Deformation factor defined by the pressure drop caused shrinkage differences in function of glass bead content and size.

FIG. 13. The ideal bead content in the function of glass bead diameter to obtain DFP = 1.

[–] are material dependent parameters, x [wt%] is the glass bead content, d_b [μm] is the glass bead diameter, and DFP_0 [–] is the deformation factor defined by the pressure drop caused shrinkage of the unfilled system.

The relation's (9) validity was proven only in the range of investigation meaning a glass bead content range of 10–40 wt%, a duration of 0.016–168 h and a glass bead size range of 11–203 μm. Table 3 contains the assessed values of the parameters featured in *Eq. 9*. By statistically evaluating the suitability of the data, the value of the correlation coefficient was (R^2) 0.94.

It can be seen that DFP can reach its optimum at a given bead content in the function of glass bead diameter (Fig. 13).

The ideal glass bead content resulting in the optimal value of deformation can be determined by a function incorporating applied bead diameter and a deformation factor, defined by the pressure drop caused shrinkage differences (DFP = 1) according to *Eq. 10*:

$$x_{id} = \frac{1 - DFP_0}{m_b \cdot d_b + m_0} \, [\text{wt\%}], \qquad (10)$$

where x_{id} [wt%] is the ideal glass bead content, m_b [–] and m_0 [–] are material dependent parameters, d_b [μm] is the glass bead diameter, and DFP_0 [–] is the deformation factor defined by the shrinkage of the unfilled material caused by the pressure drop.

CONCLUSIONS

In this article, the shrinkage and warpage properties of injection molded glass bead filled PA6 systems has been examined. The effect of altering glass bead size and con-

TABLE 3. Parameters of glass bead filled PA6 (Durethan B30S).

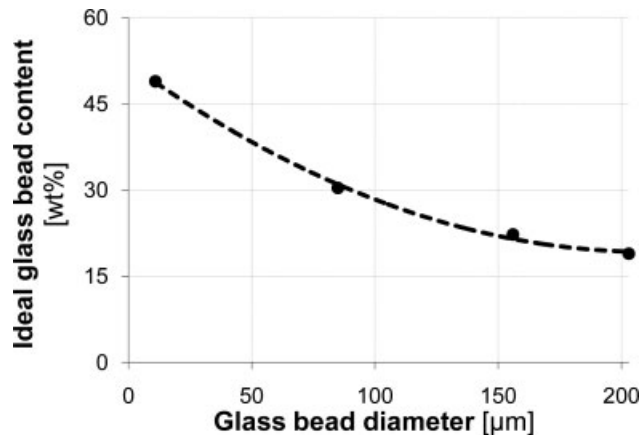| DFP_0	m_b	m_0
0.85	2.53×10^{-5}	2.79×10^{-3}

tent were investigated. Raising the glass bead content and diameter resulted in a reduction in the levels and variations of shrinkage taking place. It was concluded that the bead size did not have any effect on the near-gate cross-flow direction shrinkage but had a remarkable effect on the shrinkage at the end of the flow. This phenomenon is assumed to be caused by segregation and the inhomogeneous viscosity distribution caused by segregation. The relation between the time dependence of flow directional shrinkage and bead size and diameter was also described.

By determining the deformation factors derived from the measured shrinkages, it was pointed out that the deformation factor (DFL, *Eq. 7*) defined by the flow directional shrinkage differences was not affected by bead content or size (Fig. 10). It was demonstrated that with raising the glass bead content and decreasing bead size the DFWL factor's value could be moved to the direction of its ideal value (Fig. 11). The increase of DFP was experienced with the rise of both the glass bead content and size (Fig. 12). An equation was proposed to determine the ideal bead content in the function of applied bead diameter for reaching the optimal value of deformation factor defined by the pressure drop caused shrinkage differences.

NOMENCLATURE

A_{SL}	[–] material dependent parameter
$CaCO_3$	calcium carbonate
C_{SL}	[–] material dependent parameter
C_{SL0}	[–] constant for the unfilled material
d_b	[μm] glass bead diameter
DFL	[–] deformation factor defined by the flow directional shrinkage differences

DFP	[–] deformation factor defined by the pressure drop caused shrinkage differences
DFP$_0$	[–] deformation factor defined by the pressure drop caused shrinkage of the unfilled system
DFWL	[–] deformation factor defined by the cross-flow direction and the flow directional shrinkages
GB	glass bead
L_i	[mm] measured dimension of the specimen
L_M	[mm] dimension of the cavity
m_b	[–] material dependent parameter
m_0	[–] material dependent parameter
PA6	polyamide 6
PP	polypropylene
S_i	[%] linear shrinkage of the part
S_L	[%] average flow directional shrinkage
S_{LE}	[%] average flow directional shrinkage at the edge of the specimen
S_{L0}	[%] flow directional shrinkage in the center of the specimen
S_{L1}, S_{L2}	[%] flow directional shrinkages at the two sides of the specimen
S_{Lt0}	[%] flow directional shrinkage of the unfilled material measured 1 hour after the injection molding
$S_L(t)$	[%] flow directional shrinkage in the function of time
S_W	[%] average cross-flow direction shrinkage
S_{WE}	[%] cross-flow direction shrinkage at the end of the flow
S_{WG}	[%] cross-flow direction shrinkage near the gate
TLCP	thermotropic liquid crystalline polymer
x	[wt%] glass bead content
x_{id}	[wt%] ideal glass bead content

REFERENCES

1. K.M.B. Jansen, D.J.V. Dijk, and M.H. Husselman, *Polym. Eng. Sci.*, **38**, 838 (1998).

2. K.M.B. Jansen, G. Titomanilo, and R. Pantani, *Int. Polym. Proc.*, **12**, 4 (1997).

3. P. Postawa and J. Koszkul, *J. Mater. Process. Tech.*, **162**, 109 (2005).

4. B.H. Min, *J. Mater. Process. Tech.*, **136**, 1 (2003).

5. A. Mamat, T.F. Trochu, and B. Sanschagrin, *Polym. Eng. Sci.*, **35**, 1511 (1995).

6. K. Shelesh-Nezhad and A. Taghizadeh, *Polym. Eng. Sci.*, **47**, 2124 (2007).

7. S.J. Liao, D.Y. Chang, H.J. Chen, L.S. Tsou, J.R. Ho, H.T. Yau, W.H. Hsieh, J.T. Wang, and Y.C. Su, *Polym. Eng. Sci.*, **44**, 917 (2004).

8. J.G. Kovács, Ph.D. Thesis, *Design and Simulation of Injection Molded Products*, Budapest University of Technology and Economics (BME), Budapest (2007).

9. R.A. Malloy, *Plastic Part Design for Injection Molding*, Carl Hanser Verlag, Münich (1994).

10. J.M. Fischer, *Handbook of Molded Part Shrinkage and Warpage*, Plastics Design Library, Norwich (2003).

11. R. Thomas and N. Mccaffery, *SPE ANTEC.*, **89**, 371 (1989).

12. R.M. Shay, P.H. Foss, and C.C. Mentzer, *SPE RETEC.*, **1**, 496 (1996).

13. W.S. Depolo and D.G. Baird, *Polym. Compos.*, **27**, 239 (2006).

14. J.-Z. Liang and R.K.Y. Li, *J. Appl. Polym. Sci.*, **73**, 1451 (1999).

15. J.-Z. Liang, R.K.Y. Li, and S.C. Tjong, *Polym. Test.*, **19**, 213 (2000).

16. J.-Z. Liang, *Macromol. Mater. Eng.*, **286**, 714 (2001).

17. J.-Z. Liang, *Macromol. Mater. Eng.*, **287**, 588 (2002).

18. C.K. Huang, S.W. Chen, and C.T. Yang, *Polym. Eng. Sci.*, **45**, 1471 (2005).

19. S. Hashemi, *Express Polym. Lett.*, **2**, 474 (2008).

20. R.K.Y. Li, J.-Z. Liang, and S.C. Tjong, *J. Mater. Process Tech.*, **79**, 59 (1998).

21. J.-Z. Liang, R.K.Y. Li, and S.C. Tjong, *Polym. Test.*, **16**, 529 (1998).

22. H. Unal, *Mater. Des.*, **25**, 483 (2004).

23. S.O. Ogadhoh and T.D. Papathanasiou, *Compos. Part A-Appl. S.*, **27**, 57 (1996).

24. J.-Z. Liang and R.K.Y. Li, *J. Reinf. Plast. Comp.*, **20**, 630 (2001).

25. S.C. Jana, *Polym. Eng. Sci.*, **43**, 570 (2003).

26. J.G. Kovács and T. Tábi, *Proccedings of the Fifth Conference on Mechanical Engineering*, Budapest, **5**, 5 (2006).

27. E. Lafranche, P. Krawczak, J.-P. Ciolczyk, and J. Maugey, *Adv. Polym. Tech.*, **24**, 114 (2005).

28. E. Lafranche, P. Krawczak, J.-P. Ciolczyk, and J. Maugey, *Express Polym. Lett.*, **1**, 456 (2007).